Progress In Electromagnetics Research, Vol. 141, 33–45, 2013

A TRI-BAND IMPEDANCE TRANSFORMER USING STUBBED COUPLING LINE

Xin-Huai Wang[1, *], Li Zhang[1], Yin Xu[2], Yan-Fu Bai[1], Cheng Liu[1], and Xiaowei Shi[1]

[1]National Key Laboratory of Science and Technology on Antennas and Microwaves, Xidian University, Xi'an, Shaanxi 710071, P. R. China

[2]School of Technical Physics, Xidian University, Xi'an, Shaanxi 710071, P. R. China

Abstract—In this paper, a compact tri-band impedance transformer by utilizing stubbed coupling line for matching a load at three arbitrary frequencies is proposed. The transformer is composed of two parts, and each part is constructed from parallel-coupled transmission lines. Two structures with different configurations of the proposed transformer have been given and analyzed. Then, the close-form equations for the transformer parameters are derived analytically, and the corresponding analytical design approach is verified by numerical examples. To certify the validity of design formulas, an impedance transformer is fabricated and measured at 0.9/1.8/3.2 GHz. Good experimental performances at each frequency are obtained, which are in good agreement with the simulated results.

1. INTRODUCTION

Impedance transformers are one of the important components applied in microwave and millimeter-wave circuits, such as microwave amplifiers, power dividers, mixers, the feeding networks for a smart antenna array [1–12]. The quarter-wavelength transmission line (TL) is a conventional basic impedance transformer designed to operate at a single band. In 2002, Chow and Wan introduced a dual-band two-section 1/3-wavelength transformer operating at the fundamental frequency and its first harmonic in [7]. Then Monzon analyzed and derived its close-form solutions [8], and further proposed a small two-section dual-frequency transformer working at any two uncorrelated

Received 29 April 2013, Accepted 31 May 2013, Scheduled 9 July 2013

* Corresponding author: Xin-Huai Wang (xinhwang@mail.xidian.edu.cn).

frequencies on purely real impedance transformation [9]. An L-type impedance transformer is also developed for the same purpose in [10]. The meaningful improvements have been reported in [11], and [12], extending the impedance transformer for complex load at the third harmonics' frequency or independent frequencies. Dual-band impedances transformers are widely applied to generalized branch-line couplers, power dividers, etc. [13–23]. The growing trend towards multi-band products has increased the demand for multi-band impedance transformers. Extending from the concept of the dual-band transformer in [9], the tri-band transformers bases on three-section transmission lines for matching real impedances at three frequencies are proposed in [18], which can only work at the frequency ratio range between assigned frequency f_0 and its third harmonic. Then we present a compact quad-frequency impedance transformer composed of a two-section coupled-line to achieve ideal impedance matching four frequencies in [24]. In addition, a new analytical method to synthesize passive networks uncorrelated and unlimited number of frequencies is presented in [25]. However, it can only design to match purely imaginary loads. In recent years, researchers further focus on the areas of increasing the operating bandwidth and matching a complex impedance load [26–29].

In this paper, we propose a novel approach to match a real impedance load at three uncorrelated frequencies by using a stubbed coupling line impedance transformer. The presented transformer consists of two parts. Each part is constructed from parallel-coupled transmission lines. Two different configurations of the proposed transformer are analyzed and discussed. The design equations are carefully derived and analyzed by using transmission line theory. Furthermore, the range of frequency ratio is analytically and numerically deduced. To certify the feasibility and validity of the proposed impedance transformer, three different cases are numerically evaluated. A transformer working at 0.9 GHz/1.8 GHz/3.2 GHz is fabricated and measured to verify the proposed structure, which may be applied in the present global system for mobile communication (GSM), the personal communication (PCS) and Wi-Max. Good agreements between simulated and measured results are obtained.

2. THE STRUCTURE AND ANALYTICAL EQUATIONS

The schematic structure of the proposed tri-band transformer line is shown in Fig. 1. The circuit is simply consists of two coupled line sections **T** and **S**, which one is the transmission coupled line section **T** and the other is the stubbed coupled line section **S** shunted at the

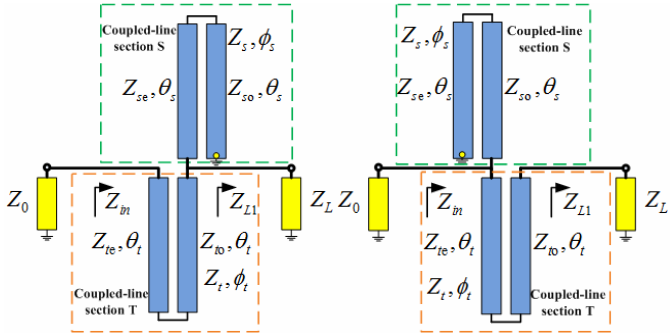

Figure 1. Structure of the proposed tri-band transformer line (a) stub at the load, (b) stub at the source.

load end (Fig. 1(a)) or at the source end (Fig. 1(b)).

As shown in Fig. 1, the coupled line section **T** and **S** odd- and even-mode characteristic impedance are Z_{te}, Z_{to} and Z_{se}, Z_{so} and the image impedance of coupled-line section **T** and coupled-line section **S** are Z_t and Z_s. The insert phase of coupled-line section **T** and coupled-line section **S** are ϕ_t and ϕ_s. According to Jones' theory in [30], here we set the two coupled line sections with the same ratio ρ ($\rho > 1$) of even- and odd-mode characteristic impedance, and the electrical lengths of the odd- and even-modes are equal. We can express the equations as following:

$$\frac{Z_{te}}{Z_{to}} = \frac{Z_{se}}{Z_{so}} = \rho \tag{1}$$

$$Z_t = \sqrt{Z_{te} \cdot Z_{to}} \tag{2}$$

$$Z_s = \sqrt{Z_{se} \cdot Z_{so}} \tag{3}$$

$$\cos\phi_t = \frac{\rho - \tan^2\theta_t}{\rho + \tan^2\theta_t} \tag{4}$$

$$\cos\phi_s = \frac{\rho - \tan^2\theta_s}{\rho + \tan^2\theta_s} \tag{5}$$

The impedance transformation ratio parameter of the source impedance and the load impedance is defined as:

$$K = \frac{Z_0}{Z_L} = \frac{Z_{in}}{Z_L} \tag{6}$$

Here, the structures in Fig. 1(a) and Fig. 1(b) are discussed respectively.

2.1. Stubbed Coupled Line Section Shunted at the Load

In Fig. 1(a), according to the transmission line theory, the input impedance Z_{in} of the two-section line is given by:

$$Z_{in} = Z_t \frac{Z'_L + jZ_t \tan\phi_t}{Z_t + jZ'_L \tan\phi_t} \tag{7}$$

$$Z'_L = \frac{jZ_s \tan\phi_s Z_L}{jZ_s \tan\phi_s + Z_L} \tag{8}$$

Applying Equation (8) to (7) and separating the real and imaginary parts, we can obtain the following equations:

$$\begin{cases} jZ_{in}Z_tZ_s \tan\phi_s = jZ_tZ_sZ_L \tan\phi_s + jZ_t^2Z_L \tan\phi_t \\ Z_{in}Z_tZ_L - Z_{in}Z_sZ_L \tan\phi_s \tan\phi_t = -Z_t^2Z_s \tan\phi_s \tan\phi_t \end{cases} \tag{9}$$

Equation (9) can be rewritten as:

$$\begin{cases} \frac{\tan\phi_t}{\tan\phi_s} = \frac{Z_{in}Z_s - Z_sZ_L}{Z_tZ_L} \\ \tan\phi_s \tan\phi_t = \frac{Z_{in}Z_tZ_L}{Z_{in}Z_sZ_L - Z_t^2Z_s} \end{cases} \tag{10}$$

To simplify the expression, let $\theta_t = \theta_s = \theta$, thus $\phi_t = \phi_s = \phi$, then we obtain:

$$\begin{cases} 1 = \frac{Z_{in}Z_s - Z_sZ_L}{Z_tZ_L} \\ \alpha \equiv \tan^2\phi = \frac{Z_{in}Z_tZ_L}{Z_{in}Z_sZ_L - Z_t^2Z_s} \end{cases} \tag{11}$$

Finally, solving Equation (11), we obtained:

$$\begin{cases} Z_t = \sqrt{Z_{in}Z_L - \frac{Z_{in}(Z_{in} - Z_L)}{\alpha}} \\ Z_s = \frac{Z_tZ_L}{Z_{in} - Z_L} \end{cases} \tag{12}$$

For $\theta_t = \theta_s = \theta$, thus $\phi_t = \phi_s = \phi$, together to solve the Equations (4), (5) and (11):

$$\begin{cases} \tan^2\theta = \rho\frac{1-\cos\phi}{1+\cos\phi} \\ \alpha = \tan^2\phi \end{cases} \tag{13}$$

By solving above equations for θ, we can obtain:

$$\theta = m\pi \pm \arctan\left(\sqrt{\rho}\tan\left(\frac{n\pi \pm \arctan\sqrt{\alpha}}{2}\right)\right) \tag{14}$$

where m, n are arbitrary integers, which means that there are four unrelated solutions. Since $\theta > 0$ and we are interested in a small transformer, we should pick the $(+)$ sign in Equation (14) when $m = n = 0$ and pick the $(-)$ sign in Equation (14) when $m = n = 1$.

Without loss of generality, we assume that $f_1 < f_2 < f_3 < f_4$, and the four fundamental solutions from Equation (14) are obtained as follows:

$$\begin{cases} \theta_1 = \arctan\left(\sqrt{\rho}\tan\frac{\arctan\sqrt{\alpha}}{2}\right) \\ \theta_2 = \arctan\left(\sqrt{\rho}\tan\frac{\pi-\arctan\sqrt{\alpha}}{2}\right) \\ \theta_3 = \pi - \arctan\left(\sqrt{\rho}\tan\frac{\pi-\arctan\sqrt{\alpha}}{2}\right) \\ \theta_4 = \pi - \arctan\left(\sqrt{\rho}\tan\frac{\arctan\sqrt{\alpha}}{2}\right) \end{cases} \tag{15}$$

where $0 < \theta_1 < \theta_2 < \theta_3 < \theta_4 < \pi$, which means that the transformer proposed in this paper can provide perfect impedance matching at four frequencies. Furthermore, we obtained the relationships from Equation (15) as following:

$$\tan\theta_1 \tan\theta_2 = \rho \tag{16}$$

$$\frac{\tan\theta_1}{\tan\theta_2} = \tan^2\left(\frac{\arctan\sqrt{\alpha}}{2}\right) \tag{17}$$

$$\theta_1 + \theta_4 = \theta_2 + \theta_3 = \pi \tag{18}$$

Applying the electrical length definition, we obtain

$$\theta_i = \beta_i l_0 = \frac{2\pi f_i}{c} l_0 \quad (i = 1, 2, 3, 4) \tag{19}$$

where c is the velocity of light, l_0 is physical length of the single coupled line.

From Equations (18) and (19), we obtain a frequency variable f_0 as follow:

$$f_0 \equiv \frac{f_1 + f_4}{2} = \frac{f_2 + f_3}{2} = \frac{c}{4l_0} \tag{20}$$

With the frequencies f_1, f_2, f_3 known, the physical length of a single coupled-line section can be calculated from Equation (20) by

$$l_0 = \frac{c}{4f_0} \tag{21}$$

And the electrical lengths θ_i, ρ and α can be calculated by

$$\theta_i = \beta_i l_0 = \frac{\pi}{2}\frac{f_i}{f_0} \quad (i = 1, 2, 3, 4) \tag{22}$$

$$\rho = \tan\left(\frac{\pi}{2}\frac{f_1}{f_0}\right)\tan\left(\frac{\pi}{2}\frac{f_2}{f_0}\right) \tag{23}$$

$$\alpha = \tan^2\left(2\arctan\sqrt{\tan\left(\frac{\pi}{2}\frac{f_1}{f_0}\right)/\tan\left(\frac{\pi}{2}\frac{f_1}{f_0}\right)}\right) \tag{24}$$

This completes the derivation of the design equations for the proposed transformer of Fig. 1(a). Obviously, seen from the circuit configuration shown in Fig. 1 and the above mentioned equations, the structure is compact, and the procedure and the equations are rigid. If the values of f_1, f_2, f_3 are known, firstly f_0 and l_0 are obtained from Equations (20) and (21), and ρ and α are calculated from Equations (23) and (24). Secondly, the image impedances Z_t and Z_s are calculated from Equation (12), and then Z_{to}, Z_{te}, Z_{so} and Z_{se} are obtained according to Equations (1)–(3). Once above design parameters are obtained, the tri-band transformer can be implemented on the special substrate directly.

2.2. Stubbed Coupled Line Section Shunted at the Source

The design solutions with the stubbed coupled line section shunted at the source as shown in Fig. 1(b) can be obtained similarly. According to the transmission line theory, the impedance matching condition for the structure is given by:

$$Z_{in} = \frac{jZ_s \tan\phi_s Z_{in1}}{jZ_s \tan\phi_s + Z_{in1}} \tag{25}$$

$$Z_{in1} = Z_t \frac{Z_L + jZ_t \tan\phi_t}{Z_t + jZ_L \tan\phi_t} \tag{26}$$

By solving the equations similarly, the solutions is obtained as follows:

$$\begin{cases} Z_t = \sqrt{Z_{in}Z_L - \frac{Z_L(Z_L - Z_{in})}{\alpha}} \\ Z_s = \frac{Z_t Z_{in}}{Z_L - Z_{in}} \end{cases} \tag{27}$$

For both these structures are the mirror of each other, the design procedure is the same as the descriptions in Section 2.1. Furthermore, it can be seen that Z_0 should be larger than Z_L in solution Equation (12) and smaller than Z_L in solution Equation (27), which means different structures for different cases.

3. ANALYSIS AND NUMERICAL SIMULATIONS

The above-mentioned solution is elementary in nature and in close form. However, it is necessary to consider the available ranges of frequency ratios in application. Here, let $f_2 = pf_1$, $f_3 = qf_2$, and $f_3 = pqf_1$, where p, q is the frequency-ratio and $1 < p < pq$. Using these in Equation (23) results in

$$\rho = \tan\frac{\pi}{p(q+1)} \tan\frac{p\pi}{p(q+1)} \tag{28}$$

Since $\rho > 1$, from Equation (25), we obtained

$$\frac{\sin\frac{\pi}{p+pq}}{\cos\frac{\pi}{p+pq}}\frac{\sin\frac{p\pi}{p+pq}}{\cos\frac{p\pi}{p+pq}} > 1 \tag{29}$$

Since $1 < p < pq$, we get $\cos\frac{\pi}{p+pq} > 0$ and $\cos\frac{p\pi}{p+pq} > 0$. After some rearrangement and using trigonometric formula, the Equation (26) can be derived as

$$\cos\frac{(p+1)\pi}{p+pq} < 0 \tag{30}$$

The solution of Equation (30) is given by

$$\frac{2-(4n+1)p}{(4n+3)p} < q < \frac{2+(1-4n)p}{(4n+1)p} \tag{31}$$

where n is an arbitrary integer. Since $1 < p < pq$, in this limit, the Equation (31) can be reduced to

$$1 < q < \frac{2+p}{p} \tag{32}$$

With this, we obtain

$$f_1 < f_2 < f_3 < 2f_1 + f_2 \tag{33}$$

Figures 2 and 3 show the relationships between the impedance ratio ρ and frequency-ratio p, q, which clearly demonstrate that the decrease rate of ρ is reducing with the increase of p and q.

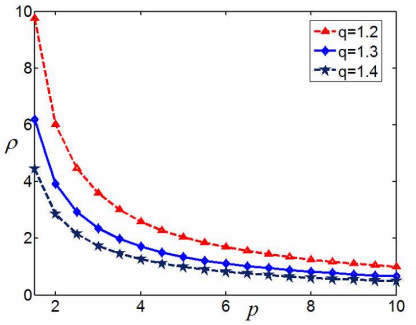

Figure 2. Relationship between ρ and frequency-ratio p.

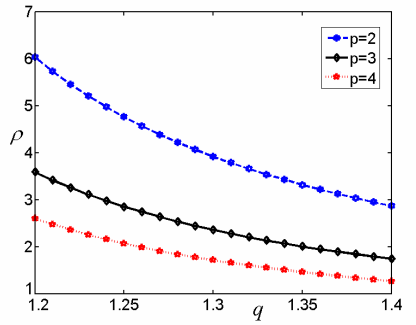

Figure 3. Relationship between ρ and frequency-ratio q.

According to the previous equations and analysis, some numerical examples are demonstrated under condition that $K = 2$. As illustrated in Table 1, f_1 and f_2 are fixed at 1 GHz and 2 GHz with $p = 2$, and f_3

and ρ varied. Fig. 4 shows the theoretical return losses as a function of ρ for fixed f_1 and $p = 2$. We can find that the return losses are well matched at three design frequencies, and the bandwidth and ρ reduce with the increase of q. Especially, when $p = 2$ and $q = 2$, ρ equals 1.00.

Table 1. Design parameters on condition $K = 2$ and $p = 2$.

	f_1 (GHz)	f_2 (GHz)	f_3 (GHz)	p	q	ρ
Case 1	1	2	2.7	2	1.35	3.31
Case 2	1	2	3.0	2	1.5	2.24
Case 3	1	2	3.3	2	1.65	1.66
Case 4	1	2	4	2	2.00	1.00

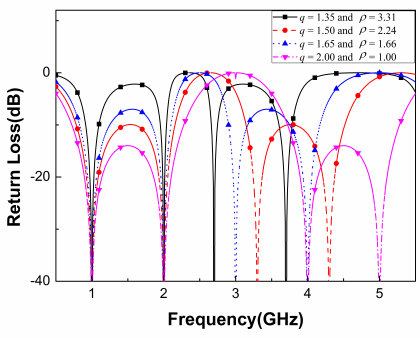

Figure 4. Theoretical return losses as a function of ρ for fixed f_1 and $p = 2$.

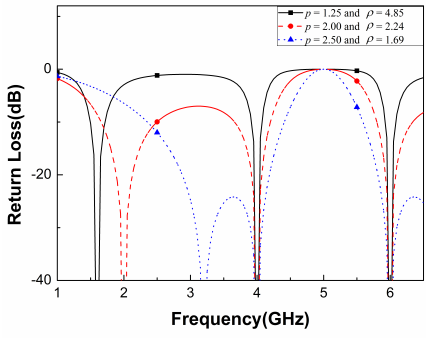

Figure 5. Theoretical return losses as a function of ρ for fixed f_3 and $q = 1.5$.

As illustrated in Table 2, f_2 and f_3 are fixed at 4 GHz and 6 GHz with $q = 1.5$, and f_1 and ρ varied. Fig. 5 shows the theoretical return losses as a function of ρ for fixed f_3 and $q = 1.5$. We can find that the return losses are well matched at three design frequencies, and the bandwidth and ρ reduce with the increase of p.

Figure 6 shows theoretical return losses as a function of K under the condition that fixed $p = 2$, $q = 3$ and $\rho = 1.66$. It is shown that the bandwidth decreases with the increase of K.

4. IMPLEMENTATION AND RESULTS

To certify the effective impedance matching at three arbitrary frequencies, a tri-band impedance transformer working at the frequencies 0.9 GHz, 1.8 GHz, and 3.2 GHz has been fabricated,

Table 2. Design parameters on condition $K = 2$ and $q = 1.5$.

	f_1 (GHz)	f_2 (GHz)	f_3 (GHz)	p	q	ρ
Case 1	3.2	4	6	1.25	1.5	3.31
Case 2	2	4	6	2.00	1.5	2.24
Case 3	1.6	4	6	2.50	1.5	1.66

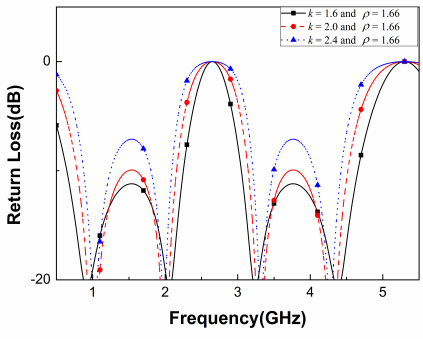

Figure 6. Theoretical return losses as a function of K for fixed $p = 2$, $q = 3$ and $\rho = 1.66$.

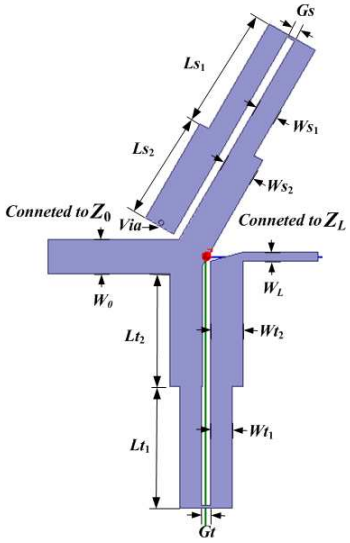

Figure 7. The model of tri-band impedance transformer with the dimension being marked.

which could be applied in GSM, PCS and Wi-MAX. The proposed transformer is designed on Taconic TLX-6 PCB ($\tan\delta = 0.0019$) with a dielectric constant of 2.65 and thickness $h = 1.0\,\text{mm}$. Here $Z_0 = 50\,\Omega$ and $Z_L = 100\,\Omega$ are chosen. As shown in Fig. 7, based on the real microstrip line, resistor and substrate, the model is built up with the dimension marked. The single section of coupled-line is replaced by stepped impedance coupled-line in model building to overcome non-TEM behavior in microstrip realization. The numerical results are calculated by Matlab 7.01, and the simulation results have been obtained by an EM simulation software Microwave Office 2004.

With the same process as that using above design procedure, we can obtain $Z_{te} = 62.99\,\Omega$, $Z_{to} = 46.70\,\Omega$, $Z_{se} = 62.99\,\Omega$ and $Z_{so} = 46.70\,\Omega$. Then the final optimum dimensions are determined as follows: $W_0 = 2.73\,\text{mm}$, $W_L = 0.7\,\text{mm}$, $Ws_1 = 1.75\,\text{mm}$, $Ls_1 = 9.63\,\text{mm}$,

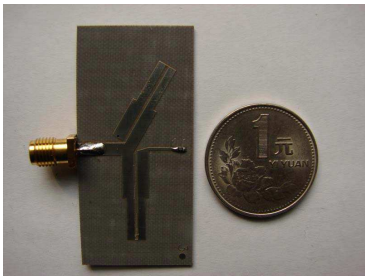

Figure 8. Photograph of the fabricated tri-band impedance transformer.

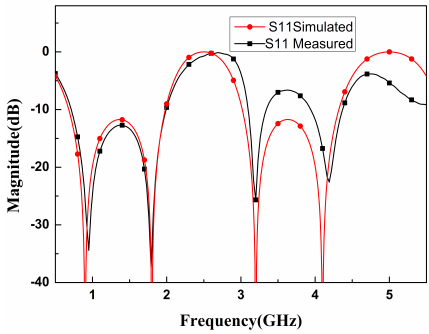

Figure 9. Simulation and measurement results of S-parameters for magnitude of S_{11}.

$Ws_2 = 2.58\,\text{mm}$, $Ls_2 = 8.59\,\text{mm}$, $Gs = 0.68\,\text{mm}$, $Wt_1 = 1.75\,\text{mm}$, $Lt_1 = 9.63\,\text{mm}$, $Wt_2 = 2.58\,\text{mm}$, $Lt_2 = 9.96\,\text{mm}$, $Gt = 0.68\,\text{mm}$.

A photograph of the fabricated impedance transformer is shown in Fig. 8. The area of the proposed impedance transformer is $2.5\times5.2\,\text{cm}^2$.

All the measured data are collected from the Agilent N5230A network analyzer. Fig. 9 demonstrates the measured and simulated results of return-loss. The measured results of the return loss are about $-25.7\,\text{dB}$ at $0.9\,\text{GHz}$, $-34.3\,\text{dB}$ at $1.8\,\text{GHz}$, and $-25.6\,\text{dB}$ at $3.2\,\text{GHz}$, respectively. It is seen that the measured results are in good agreement with simulated ones for the load at the assigned frequencies. Some slight differences at higher frequency between measured and simulated results may be due to serious parasitic effects arisen from via holes, soldering, and the limited precision of fabrication and measurement.

5. CONCLUSION

A novel tri-band impedance transformer is presented in this paper. By using stubbed coupling line, the proposed transformer line can match a real impedance load at three uncorrelated frequencies and can shorten the horizontal length. Two structures with two different configurations of the proposed transformer have been given and analyzed. Design equations are analytically derived, and the range of frequency ratio is numerically deduced for the transformer parameters. The numerical examples are evaluated to certify the feasibility of the proposed impedance transformer. In addition, a transformer operating at $0.9\,\text{GHz}/1.8\,\text{GHz}/3.2\,\text{GHz}$ is fabricated and measured to verify the proposed structure, which may be applied in the present global system

for mobile communication (GSM), the personal communication system (PCS) and Wi-Max. The measured results show good agreements with the simulated ones. The tri-band transformer could be widely applied in compact multi-band component including power dividers, couplers and antennas' matching.

ACKNOWLEDGMENT

This work was supported by the fundamental research funds for the Central Universities (K50511020021) and the National Natural Science Foundation of China under Grant 61201298.

REFERENCES

1. Moon, B.-T. and N.-H. Myung, "A dual-band impedance transforming technique with lumped elements for frequency-dependent complex loads," *Progress In Electromagnetics Research*, Vol. 136, 123–139, 2013.
2. Castaldi, G., V. Fiumara, and I. Gallina, "An exact synthesis method for dual-band chebyshev impedance transformers," *Progress In Electromagnetics Research*, Vol. 86, 305–319, 2008.
3. Shamaileh, K. A. A., A. M. Qaroot, and N. I. Dib, "Non-uniform transmission line transformers and their application in the design of compact multi-band bagley power dividers with harmonics suppression," *Progress In Electromagnetics Research*, Vol. 113, 269–284, 2011.
4. Lin, X., P. Su, Y. Fan, and Z. B. Zhu, "Improved CRLH-TL with arbitrary characteristic impedance and its application in hybrid ring design," *Progress In Electromagnetics Research*, Vol. 124, 249–263, 2012.
5. Shamaileh, K. A. A., A. M. Qaroot, and N. I. Dib, "Non-uniform transmission line transformers and their application in the design of compact multi-band bagley power dividers with harmonics suppression," *Progress In Electromagnetics Research*, Vol. 113, 269–284, 2011.
6. Wu, Y. and Y. Liu, "An unequal coupled-line Wilkinson power divider for arbitrary terminated impedances," *Progress In Electromagnetics Research*, Vol. 117, 181–194, 2011.
7. Chow, Y. L. and K. L. Wan, "A transformer of one-third wavelength in two sections for a frequency and its first harmonic," *IEEE Microwave and Wireless Components Letters*, Vol. 12, 22–23, 2002.

8. Monzon, C., "Analytical derivation of a two section impedance transformer for a frequency and its first harmonic," *IEEE Microwave and Wireless Components Letters*, Vol. 12, No. 10, 381–382, 2002.
9. Monzon, C., "A small dual-frequency transformer in two sections," *IEEE Trans. Microw. Theory Tech.*, Vol. 51, No. 4, 1157–1161, Apr. 2003.
10. Park, M.-J. and B. Lee, "Dual-band design of single-stub impedance matching networks with application to dual-band stubbed T-juctions," *Microwave and Optical Technology Letters*, Vol. 52, No. 6, 1359–1362, 2010.
11. Colantonio, P., F. Giannini, and L. Scucchia, "A new approach to design matching networks with distributed elements," *15th International Conference on Microwaves, Radar and Wireless Communications, MIKON-2004*, Vol. 3, Nos. 17–19, 811–814, 2004.
12. Scucchia, L., "Closed-form approach to design distributed matching networks for high-frequency amplifiers," *Int. J. of RF and Microwave Computer-aided Engineering*, Vol. 16, No. 4, 374–384, Jul. 2006.
13. Cheng, K.-K. M. and C. Law, "A new approach to the realization of a dual-band microstrip filter with very wide upper stopband," *IEEE Trans. Microw. Theory Tech.*, Vol. 56, No. 6, 1461–1467, 2008.
14. Wang, X.-H., D. Chen, X. Shi, F. Wei, and X. Chen, "A compact three-way dual frequency power divider," *Microwave and Optical Technology Letters*, Vol. 51, No. 4, 2009.
15. Wu, Y., Y. Liu, Y. Zhang, J. Gao, and H. Zhou, "A dual band unequal wilkinson power divider without reactive components," *IEEE Trans. Microw. Theory Tech.*, Vol. 57, No. 1, 216–222, 2009.
16. Park, M.-J. and B. Lee, "A dual-band Wilkinson power divider," *IEEE Microwave and Wireless Components Letters*, Vol. 18, No. 2, 85–87, 2008.
17. Wang, X. H., L. Chen, X. W. Shi, Y. F. Bai, L. Chen, and X. Q. Chen, "Planar dual-frequency power divider using umbrella-shaped resonator," *Journal of Electromagnetic Waves and Applications*, Vol. 24, Nos. 5–6, 597–606, 2010.
18. Chongcheawchamnan, M., S. Patisang, S. Srisathit, R. Phromloungsri, and S. Bunnjaweht, "Analysis and design of a three-section transmission-line transformer," *IEEE Trans. Microw. Theory Tech.*, Vol. 53, No. 7, 2458–2462, Jul. 2005.

19. Bai, Y. F., X. H. Wang, C. J. Gao, Q. L. Huang, and X. W. Shi, "Design of compact quad-frequency impedance transformer using two-section coupled line," *IEEE Trans. Microw. Theory Tech.*, Vol. 60, 2417–2423, 2012.
20. Giofre, R., P. Colantonio, F. Giannini, and L. Piazzon, "A new design strategy for multi frequencies passive matching networks, *Proc. Eur. Microw. Conf.*, 838–841, Oct. 2007.
21. Liu, X., Y. Liu, S. Li, F. Wu, and Y. Wu, "A three-section dual-band transformer for frequency-dependent complex load impedance," *IEEE Microwave and Wireless Components Letters*, Vol. 19, No. 10, 611–613, Oct. 2009.
22. Nikravan, M. A. and Z. Atlasbaf, "T-section dual-band impedance transformer for frequency-dependent complex impedance loads," *Electron. Lett.*, Vol. 47, No. 9, 551–553, Apr. 2011.
23. Jones, E. M. T., "Coupled-strip-transmission-line filters and directional couplers," *IRE Trans. Microwave Theory Tech.*, Vol. 4, No. 2, 75–81, Apr. 1956.
24. Bai, Y. F., X. H. Wang, C. J. Gao, Q. L. Huang, and X. W. Shi, "Design of compact quad-frequency impedance transformer using two-section coupled line," *IEEE Trans. Microw. Theory Tech.*, Vol. 60, 2417–2423, 2012.
25. Giofre, R., P. Colantonio, F. Giannini, and L. Piazzon, "A new design strategy for multi frequencies passive matching networks," *Proc. Eur. Microw. Conf.*, 838–841, Oct. 2007.
26. Moon, B.-T. and N.-H. Myung, "A dual-band impedance transforming technique with lumped elements for frequency-dependent complex loads," *Progress In Electromagnetics Research*, Vol. 136, 123–139, 2013.
27. Wu, Y., W. Sun, S.-W. Leung, Y. Diao, and K.-H. Chan, "A novel compact dual-frequency coupled-line transformer with simple analytical design equations for frequency-dependent complex load impedance," *Progress In Electromagnetics Research*, Vol. 134, 47–62, 2012.
28. Liu, Y., Y.-J. Zhao, and Y. Zhou, "Lumped dual-frequency impedance transformers for frequency-dependent complex loads," *Progress In Electromagnetics Research*, Vol. 126, 121–138, 2012.
29. Nikravan, M. A. and Z. Atlasbaf, "T-section dual-band impedance transformer for frequency-dependent complex impedance loads," *Electron. Lett.*, Vol. 47, 551–553, 2011.
30. Jones, E. M. T., "Coupled-strip-transmission-line filters and directional couplers," *IRE Trans. Microwave Theory Tech.*, Vol. 4, No. 2, 75–81, Apr. 1956.